

# STUDY OF TRAPPED MAGNETIC FLUX IN SUPERCONDUCTING NIOBIUM SAMPLES

S. Aull\*, O. Kugeler, J. Knobloch, Helmholtz-Zentrum Berlin, Germany

## Abstract

Trapped magnetic flux is known to be one cause of residual losses in bulk niobium SRF cavities. In the Meissner state an ambient magnetic field should be expelled from the material. Disturbances such as lattice defects or impurities have the ability to inhibit the expulsion of an external field during the superconducting transition so that the field is trapped.

We measured the fraction of trapped magnetic flux in niobium samples with different treatment histories, such as BCP and tempering. The differences between single crystal and polycrystalline material as well as the influence of spatial temperature gradients and different cooling rates were investigated. In addition, the progression of the release of a trapped field during warm up was studied.

## INTRODUCTION

The surface resistance defines the dissipated power in an SRF cavity. It consists basically of two contributions. The BCS contribution described by the BCS theory decreases exponentially with temperature and depends additionally on the operating frequency.

In addition to the BCS contribution there is a residual resistance which is temperature independent. At a typical operating temperature of 2 K, the residual resistance accounts for 10 to 30 % of the total surface resistance [1].

SRF cavities are operated in the Meissner state so an external magnetic field should be expelled from the material. Imperfections of the crystal lattice like impurities, dislocations and grain boundaries have the ability to suppress the expulsion of magnetic field during the superconducting transition. The field remains in the material even after switching off the source of the external magnetic field.

This trapped field penetrates the material in the form of flux tubes which have a normal conducting core. The unpaired electrons in this normal conducting areas cause an ohmic resistance and therefore account for the (residual) surface resistance.

The residual resistance increases linearly with the trapped field and depends on the operating frequency:

$$R_{\text{res}} = \alpha H_{\text{trap}} \sqrt{f/\text{GHz}} \quad (1)$$

$\alpha$  describes the sensitivity of the surface resistance on the trapped field. It has to be determined experimentally, e.g. reference [2] found  $\alpha = 2.2 \frac{\text{n}\Omega}{\mu\text{T}}$ .

At 1.3 GHz the additional surface resistance due to trapped flux would be 125 n $\Omega$  if no magnetic shielding is provided and the earth magnetic field of about 50  $\mu\text{T}$  is trapped completely. In the early 90's, Vallet et al. already measured 100 % flux trapping when exposing niobium to external fields up to 300  $\mu\text{T}$  [3].

At 2 K and 1.3 GHz, the surface resistance can be as high as 15 n $\Omega$  [4]. If a magnetic shield with 95 % efficiency is used, then the earth's field would account for nearly half of this residual resistance (6.3 n $\Omega$ ).

The flux trapping mechanisms are predominantly studied in the Shubnikov phase of type II superconductors where it is energetically favorable when an ambient magnetic field penetrates the material. In the Shubnikov phase the magnetic field forms a hexagonal lattice of quantized flux tubes. A lot of calculations were done, estimating the interaction between the flux tube lattice and the variation in the lattice defects distribution. Pinning forces of different kinds of pinning centers, the interaction between the flux tubes themselves as well as the coexistence of normal conducting and superconducting areas (*intermediate state*) are subjects of the recent studies. An overview on these topics can be found in reference [5].

The goal of these experiments was to study the flux trapping (in the Meissner phase) in representative niobium samples to better understand the impact of treatment history and operating conditions on flux trapping.

Moreover, past measurements suggest that thermal gradients will generate currents by the Seebeck effect whose magnetic field can be trapped during the superconducting transition [6]. A further goal of these measurements was to study this effect in more detail.

## EXPERIMENT

### Set-up

We constructed a scanning device capable of generating trapped flux in niobium discs and scanning the field with the niobium in the superconducting state. The setup was installed in the HoBiCaT facility [7].

Figure 1 shows the top view onto the sample holder made from copper. The niobium samples are located under the rectangular copper covers. It provides four sample positions and is cooled to 6 – 8 K.

Two heater foils serve as heat sources in order to quickly cycle the samples between normal and superconducting state without warming up the whole cryostat.

\* sarah.aull@helmholtz-berlin.de

The field measurements were done with a fluxgate magnetometer able to operate at cryogenic temperatures. It could be moved into the two lateral directions which enables measurements of four samples and scanning the field over each sample.

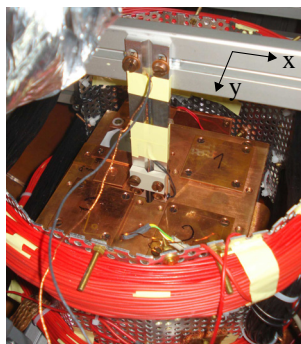


Figure 1: Set-up to scan trapped flux in Nb samples.

The external magnetic fields up to 2.3 mT were generated by a pair of Helmholtz coils which were placed above and below the sample holder.

A detailed description and characterization of the measurement device can be found in reference [8].

### Samples

The niobium samples differ in crystal structure and in their treatment history. Tempering at different temperatures dissolves hydrogen (800°C) and light elements (1200°C) and homogenizes the material.

The *Buffered Chemical Polishing* (BCP) removes the surface layer which is damaged during the fabrication process. In case of tempered samples an additional BCP was done after tempering.

The samples are discs of 37 – 48 mm diameter and have 2.6 – 3.1 mm thickness.

Table 1: List of measured samples – all samples had an RRR of about 260 before the treatment.

Sample	Crystal Structure	Treatment
1	polycrystalline	–
2	polycrystalline	BCP
3	polycrystalline	BCP + 800°C
4	single crystal	BCP
5	single crystal	BCP + 800°C
6	single crystal	BCP + 1200°C

### Measurement Procedure

Trapping a magnetic field proceeds as follows:

- the sample is warmed up in the normal conducting state ( $T > T_c$ )
- the Helmholtz coils are switched on, applying a magnetic field  $B_{\text{applied}}$
- the sample is cooled to the superconducting state ( $T < T_c$ )
- the Helmholtz coils are switched off
- the field probe measures any remaining field which is considered to be the trapped magnetic field  $B_{\text{trapped}}$

As the field probe measures the magnetic field at a certain distance above the sample, the field on the sample surface has to be calculated. This is outlined in the following section.

### Field Simulation

We simulated the magnetic field of a uniformly magnetized disc and calculated the field at a certain distance above the disc's surface which corresponds to the distance between the field probe and the sample surface.

Figure 2 compares the magnetic field at the probe position as a function of the radial position with the measured magnetic field. The comparison of the measured lateral profile with the simulated one confirms that the assumption of a uniformly magnetized disc within the resolution of the sensor is reasonable.

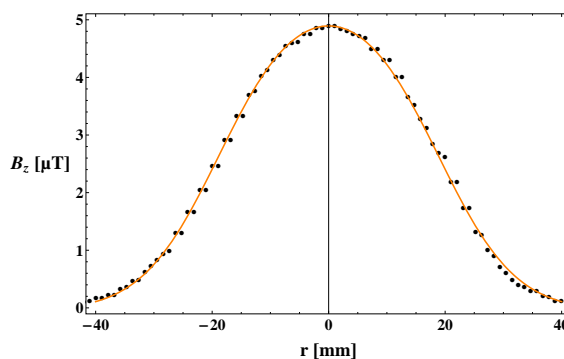


Figure 2: Calculated magnetic field of a homogeneously magnetized disc at the probe position compared to the measured trapped field as a function of the radius.

## RESULTS

### Influence of Treatment and Field Strength

All samples were exposed to ambient fields up to 300  $\mu\text{T}$ . Additionally, ambient fields up to 2.3 mT were applied to the untempered polycrystalline samples (Samples 1 and 2).

It was observed that each sample traps a fixed fraction of the applied field independent of the strength of the applied field.

The fraction of the trapped field on the surface was calculated from the measured data. The total fraction of trapped field for each sample can be found in Table 2.

The fraction is greatest for untempered polycrystalline samples (100 %) and least for heat-treated single crystal samples (ca. 40 %).

### Influence of the Cooling Rate

The fraction of trapped magnetic field was also measured as a function of the cooling rate  $v$ . Cooling rates in the range of 0.5 – 60 mK/s could be produced.

A logarithmic dependency on the cooling rate was found for all single crystal samples. Polycrystalline samples

Table 2: Flux trapping behavior of all measured samples. Only single crystal samples showed a dependence on the cooling rate  $\nu$  (in mK/s).

Sample	Crystal Structure	Treatment	Fraction of Trapped Flux
1	polycrystalline	–	100%
2	polycrystalline	BCP	100%
3	polycrystalline	BCP + 800°C	$(83.1 \pm 0.8) \%$
4	single crystal	BCP	$[(72.9 + 0.1 \ln \nu) \pm 0.8] \%$
5	single crystal	BCP + 800°C	$[(61.6 + 1.3 \ln \nu) \pm 0.8] \%$
6	single crystal	BCP + 1200°C	$[(42.1 + 0.13 \ln \nu) \pm 0.6] \%$

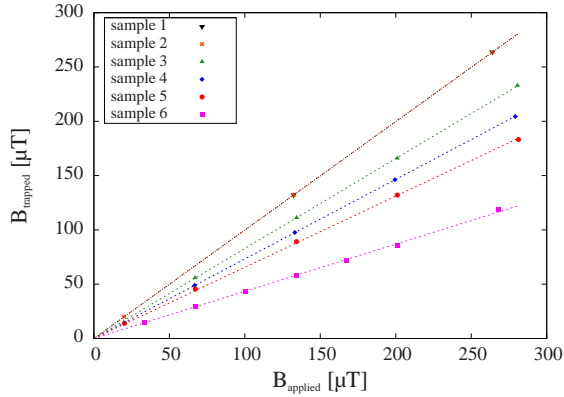


Figure 3: Dependency of the trapped field on the applied field for all measured samples: None of the samples exhibited a saturation of the trapped field.

showed no dependence. Figure 4 shows exemplarily the fraction of trapped field as a function the cooling rate for the 800°C tempered single crystal sample.

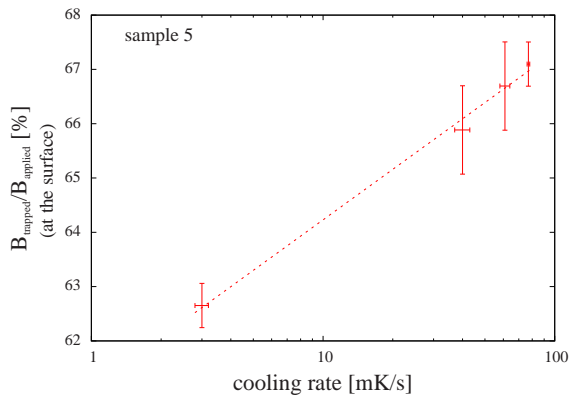


Figure 4: Dependency of the trapped field on the cooling rate for a single crystal sample with 800°C tempering.

*Flux Release*

Additionally, the transition from the superconducting to the normal conducting state and the associated release of trapped flux was examined. For that purpose, a sample with

a trapped field was warmed up very slowly until the trapped field vanished.

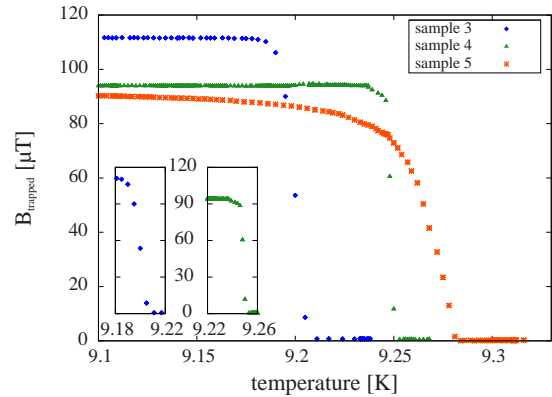


Figure 5: Release of the trapped field during warm up: The tempered single crystal samples released the trapped field over a broad temperature range.

Figure 5 shows the release of a trapped field for the samples 3, 4 and 5. It was observed that the tempered single crystal samples release the trapped fields within a broad temperature range. For all other samples the transition was significantly less broad. The narrowest transition is observed with polycrystalline niobium.

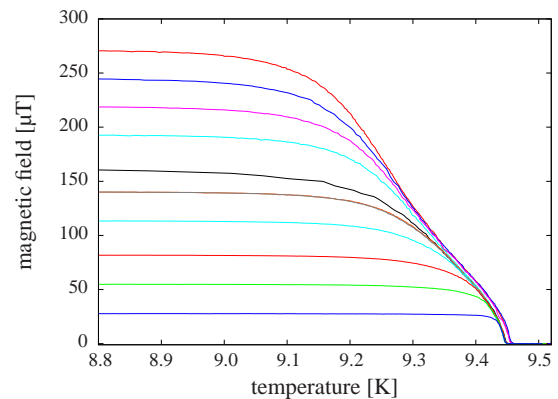


Figure 6: Release of different trapped fields during warm up for a single crystal sample with 1200°C tempering.

Figure 6 shows the progression of the flux release for different trapped fields. It can be seen that the higher the trapped field is the lower is the temperature where the release starts. Nevertheless, the progression near  $T_c$  is the same.

We found that during the flux release the sample was still fully in the superconducting state by the following test: During the release the heater was turned off so that the samples cooled down again. Simultaneously, the Helmholtz coils were switched on again. After reaching the cool equilibrium temperature, the level of trapped field was measured.

It was found that the level of trapped field is the level of field at the moment the heating was aborted. No additional flux was trapped due the applied field and it can be concluded that the sample was therefore completely superconducting.

### Thermal Currents

One of the sample positions was designed in such a way that it allowed the generation of a spatial temperature gradient of about 0.5 K/cm over the sample.

Due to the thermo-electric effect (Seebeck effect) a temperature gradient produces a thermal current and therefore an additional magnetic field (*Seebeck field*). We were able to confirm the existence of such a field at cryogenic temperatures when the sample was above  $T_c$ .

Unfortunately, the measured strength of the Seebeck field was of the same order as the generated field by the heater used to establish the thermal gradient. To separate out the effect, the experiment was repeated twice with opposite polarity of the heater, but the same power. The difference of the magnetic field measurement then yields the Seebeck field since the magnetic field due to thermal currents does not change the orientation when the heater current is reversed.

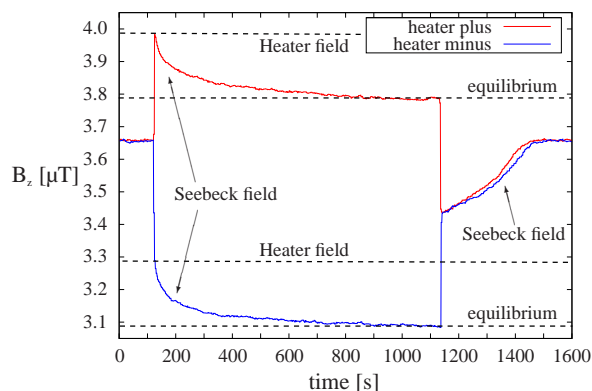


Figure 7: Progression of the magnetic field due to the Seebeck effect superimposed with the heater fields for both current directions. The heater was switched on  $t = 120$ s to establish a temperature gradient. It was switched off at  $t = 1120$ s.

Figure 7 depicts the measured magnetic field which is a superposition of the constant field produced by the heater and the field induced by the thermal current as long the heater is switched on. After switching on the heater a negatively oriented field builds up due to the rising temperature gradient, superposing the constant heater field. After switching off the heater ( $t > 1120$ s) there is no heater field and the decrease of the pure Seebeck field can be observed.

Furthermore, it was found that the thermal current has an impact on the trapping behavior of the sample. A quantitative analysis has not yet been completed and will be the subject of future investigations.

## CONCLUSION

The measurements showed that the treatment history of the niobium samples has a great influence on the trapping behavior. The *fraction* of trapped flux seems to depend on the impurity content and especially on the number of grain boundaries. By contrast, no influence of the strength of the applied field or the BCP was found.

Additionally, the release of the trapped field over a broad temperature range was observed for the tempered single crystal samples although the samples were shown to be superconducting during the flux release near  $T_c$ . These are the samples that exhibited the least amount of flux trapping and hence must have weaker pinning centers. One speculation is that their pinning strength decreases further with temperature as  $T_c$  is approached, leading to gradual flux release. This will be the subject of future measurements.

Moreover, it could be shown that a local temperature gradient induces an additional magnetic field.

## ACKNOWLEDGMENTS

We would like to thank Peter Kneisel (Jefferson Laboratory), Peter vom Stein (RI), Enzo Palmieri (INFN) and Rong-Li Geng (Jefferson Laboratory) for providing all samples.

Moreover, we thank to Andre Frahm (HZB) for the construction of the measurement device.

## REFERENCES

- [1] P. Schmüser, "Superconductivity", CAS 2003: Superconductivity and Cryogenics for Accelerators and Detectors, 2003.
- [2] P. Kneisel and B. Lewis, "Additional RF - Surface Resistance in Superconducting Niobium Cavities Caused by Trapped Magnetic Flux", Tech. Note 94 - 028, 1994.
- [3] C. Vallet *et al.*, "Flux Trapping in Superconducting Cavities", EPAC proc. 1992, p. 1295.
- [4] B. Aune *et al.*, "Superconducting TESLA Cavities", PR ST AB, Vol. 3, 2000.
- [5] R. P. Huebener, "Magnetic Structures in Superconductors", Springer, 2001, ISBN 3540092137.
- [6] J. Knobloch and H. Padamsee, "Flux trapping in niobium cavities during breakdown events", Proc. of the 1997 Workshop on RF Superconductivity.

- [7] O. Kugeler, A. Neumann, W. Anders and J. Knobloch, "Adapting TESLA technology for future cw light sources using HoBiCaT", Rev. Sci. Instrum. 81, 2010.
- [8] S. Aull, "Investigation of trapped magnetic flux in superconducting niobium samples", Diplomarbeit, Institut für Physik, Humboldt Universität zu Berlin, 2010